Supporting Information

Schimel et al. 10.1073/pnas.1407302112

SI Materials and Methods

Output from nine land surface/terrestrial biosphere models was used in this analysis (Table S1). This study made use of TRENDY terrestrial process and RECCAP atmospheric inverse model results (www.globalcarbonproject.org/reccap) downloaded in March 2014. The model runs were contributed to the TRENDY model intercomparison project using common input/forcing data. The models included: CLM4-CN (1), HYLAND (2), LPJwsl (3), LPJ-GUESS (4), OCN (5), ORCHIDEE (6), SDGVM (7), TRIFFID (8), and VEGAS (9). Model simulations were conducted over the years 1860–2010 with three experiments varying: (*i*) CO_2 only (S1: time-invariant climate; present day land use mask); (*ii*) CO_2 and climate (S2: present-day land use mask); and (*iii*) CO_2, climate, and land use (3). Only five of the TRENDY models submitted results for the S3 experiment including CO_2, climate, and land use forcings (HYLAND, LPJ, OCN, ORCHIDEE, VEGAS), and thus only these models are shown in Fig. 3 and Fig. S1.

The TRENDY models were driven primarily with Climate Research Unit plus National Centers for Environmental Prediction (CRU+NCEP) climate forcing data for 1901–2010 (10), downloaded at dods.extra.cea.fr/data/p529viov/cruncep/ through dgvm.ceh.ac.uk/node/9 (11–13). The CRU+NCEP data are a combination of two existing datasets: (*i*) the CRU TS.3.1 0.5° × 0.5° monthly climatology covering the period 1901–2009 and (*ii*) the US National Oceanic and Atmospheric Administration (NOAA) NCEP and National Center for Atmospheric Research (NCAR) reanalysis 2.5° × 2.5° 6-hourly climatology covering the period 1948 to near real time.

We used only the S1 simulations to produce Figs. 1 and 2. For Fig. 1, we calculated zonal sums for the CO_2 effect on carbon uptake and GPP for each model and experiment. For this the global flux grid (kilograms carbon per square meter per year) was multiplied by land area (square meters) at every pixel. Then, the sum of total fluxes by latitude was calculated (kilograms carbon per year per degree) and converted to petagrams for a final output in petagrams carbon per year per degree. The spatial resolutions differed among models (Table S1), so we converted all finer-resolution models to the latitude resolution of the coarsest model, which was 2.5 degrees, maintaining consistency in total surface area. We also calculated the multimodel ensemble mean and SD, with the SD plotted as a gray shaded area plus/minus around the black mean line in Fig. 1.

In Fig. 2, the net terrestrial sink is calculated by subtracting the atmospheric concentration increase and estimated ocean uptake from the estimated historical fossil fuel emissions as described in Le Quéré et al. (14) and inherently includes both land use and undisturbed land (CO_2 and other effects) contributions. The effect of increasing CO_2 concentration shown is the multimodel mean effect from TRENDY, varying CO_2 and holding climate and land use constant (see supplementary material). The TRENDY and GCP data were averaged to 10-y intervals. By convention, CO_2 uptake from the atmosphere is negative, but is plotted inverted here to aid comparison with CO_2 concentration. CO_2 concentration data come from the Law Dome record [1850–1957; cdiac.ornl.gov/trends/co2/lawdome-data.html (15)] stitched onto Scripps Mauna Loa data [1958–2013; scrippsco2.ucsd.edu (16)] with the Law Dome record adjusted for the interhemispheric gradient. The Law Dome data were shifted +0.4 ppm to match the Mauna Loa Observatory record in 1958, with the adjustment decreasing (scaled by fossil fuel emissions) to +0.01 ppm in 1850.

For the atmospheric inversion and the in situ inventory-based flux estimates, we show previously published results in Fig. 3. The TransCom 3 atmospheric tracer transport model intercomparison project included several experiments comparing collections of CO_2 inverse models under prescribed conditions (Table S2). This project is described extensively online (transcom.project.asu.edu) and in ref. 17. Gurney et al. (17) first reported model ensemble means with strong northern and weak tropical uptake from an experiment with fixed seasonal flux cycles. We present results here from the Level 2 experiment that solved for seasonally varying fluxes (17). This experiment included 12 models and estimated fluxes for the 1992–1996 period. To isolate the effect of transport differences, the models all used the same set of observational data, presubtracted fossil fuel fluxes, prior ocean and terrestrial fluxes and uncertainties, and inversion methodology.

The Stephens et al. (18) study compared posterior CO_2 concentration fields from these models to observations of vertical CO_2 distributions in the northern midlatitudes and concluded that biases in vertical transport led most models to overestimate northern and underestimate tropical CO_2 uptake. Although no models reproduced vertical gradients in all seasons, this study used the three models with the best annual mean gradients to derive the subset flux estimate shown in Fig. 3 and Fig. S1.

The more recent RECCAP atmospheric inverse model intercomparison study (19) included 11 models and reported fluxes over a common 2001–2004 period (Table S3). These models, in general, operate at higher spatial resolution and use larger collections of CO_2 observations than those in T3L2. Thus, it is possible that transport biases or their impact may have been reduced. However, the spread in these models is still significant. In contrast to T3L2, the RECCAP models did not follow a set protocol and used different collections of observational data, and different error characterization and flux estimation techniques. These differences likely contribute to the model spread. However, it is possible that differences in vertical transport still play a primary role in determining the northern versus tropical flux distributions. The RECCAP study did not collect posterior concentration fields, nor were these produced or archived by many of the participating groups, so we were not able to recreate the comparison with vertical gradients done by Stephens et al. (18). The RECCAP results shown here correspond to the final version of the Peylin et al. (19) study (Table S3), and, as described in that paper, for five models, these results may differ from those used in other RECCAP synthesis papers and the discussion version of the Peylin et al. (19) paper.

Results from Pan et al. (20) including uncertainties were taken directly from the publication (their table 1). Pan et al. (20) did not separate northern extratropical fluxes into deforestation, intact forests, and regrowing forests, and therefore the northern extratropical net flux is shown. Pan et al. (20) included the total uptake for Australia and New Zealand (-0.06 Pg $C{\cdot}y^{-1}$ for both decades) in their temperate estimate. Here we subtract this value from their temperate number and add it in to our tropical+southern intact forest estimate for comparison with the atmospheric inverse estimates.

The uncertainties in Pan et al. (20) require some additional discussion. Pan et al. present estimates for three time periods, 1990–1999, 2000–2007, and 1990–2007 inclusive. There are other estimates for some of the tropical fluxes and part of this time period (2000–2005). For a detailed discussion, see Harris et al. (21) and Tollefson (22). None of these reports compile a complete tropical carbon budget, and they span a shorter time period, but they attempt to reconcile different approaches to reporting tropical land use fluxes relative to emission reduction targets. The remote sensing-based estimates of tropical carbon (23) may suggest lower losses of carbon because of lower biomass estimates (which would lead to the deforestation vector in Fig. 3 and Fig. S1 becoming shorter), but if biomass is systematically overestimated by in situ methods as they suggest, that would also reduce the magnitude of the regrowth and growth in intact forest vectors. Since none of these reports provide the complete carbon budget (including the northern hemisphere) that Pan et al. does, we can only suggest that the remote sensing (23) analyses be extended globally to be consistent with our approach of explicit reconciliation of atmospheric and biomass and land use activity approaches. Since none of these recent analyses provide complete budgets, we cannot incorporate their fluxes and uncertainties into this analysis, other than to suggest there may be another solution with somewhat smaller tropical flux components and thus a somewhat smaller estimate of the CO_2 effect.

The T3L2, RECCAP, and TRENDY results shown in Fig. 3 and Tables S1, S2, and S3 have been divided into tropical+ southern and northern extratropical regions according to the TransCom/RECCAP flux regions. The tropical+southern land fluxes are a sum of fluxes from the Tropical America, Northern Africa, Tropical Asia Temperate South America, Southern Africa, and Australia regions, while the northern extratropical land fluxes are a sum of fluxes from the Boreal North America, Temperate North America, Boreal Asia, Temperate Asia, and Europe regions. The TRENDY results used to calculate the best estimate budget presented in the text and in Table 1 have also been aggregated by the TransCom/RECCAP regions.

For the 1990–2007 combined flux estimates in the lower two rows of Table 1, we calculate weighted averages of Pan et al. (20) and TRENDY results. The individual northern extratropical uptake estimates are -1.16 ± 0.16 (20) and -1.14 ± 0.22 (TRENDY S3 experiment median and SD of five models), giving a weighted average of $([-1.16/0.16] - [1.14/0.22])/([1/0.16] + [1/0.22]) = -1.15 \pm 0.13$. The individual tropical+southern CO_2 effect estimates are -1.25 ± 0.41 [Pan et al. (20) tropical intact forest] and -1.56 ± 0.66 (TRENDY S1 experiment median and SD of nine models), giving a weighted average of $([-1.25/0.41] - [1.56/0.66])/([1/0.41] + [1/0.66]) = -1.37 \pm 0.36$. For the global CO_2 effect estimate, we add this tropical+southern CO_2 effect number (-1.37 ± 0.36) to the TRENDY northern extratropical number of -1.08 ± 0.44 (S1 experiment median and SD of nine models) to get -2.45 ± 0.57, adding errors in quadrature. All units are in petagrams carbon per year.

Note that Table 1, being built from "bottom-up" flux estimates, reconciled with mass balance and top-down estimates, does not contain a residual terrestrial flux forced to balance the budget and so does not balance exactly to zero. The budget balances within the uncertainty of the other flux estimates and is out of exact balance by 0.3 $Pg{\cdot}y^{-1}$ ($\pm$1.0). We also assign a bottom-up estimate of the uncertainty, and by bringing additional information into the budget from models, forest inventory, the mass balance, and Stephens et al. (18) constraints, reduce the overall uncertainty of the budget, compared with a budget with a residual terrestrial flux, with uncertainty estimated from quadrature of the other flux uncertainties. The 0.3 $Pg{\cdot}y^{-1}$ residual is the arithmetic equivalent of the residual terrestrial flux but could represent a small systematic error or combination of errors in any of the terms, fossil, ocean, or terrestrial. Given the limited data, a balanced, bottom-up, budget would be unexpected.

1. Thornton PE, Lamarque J-F, Rosenbloom NA, Mahowald NM (2007) Influence of carbon-nitrogen cycle coupling on land model response to CO_2 fertilization and climate variability. *Global Biogeochem Cycles* 21:1–15.
2. Levy PE, Cannell MGR, Friend AD (2004) Modelling the impact of future changes in climate, CO_2 concentration and land use on natural ecosystems and the terrestrial carbon sink. *Glob Environ Change* 14:21–30.
3. Sitch S, et al. (2003) Evaluation of ecosystem dynamics, plant geography and terrestrial carbon cycling in the LPJ dynamic global vegetation model. *Glob Change Biol* 9:161–185.
4. Smith B, Prentice IC, Sykes MT (2010) Representation of vegetation dynamics in modelling of terrestrial ecosystems: Comparing two contrasting approaches within European climate space. *Glob Ecol Biogeogr* 10:621–637.
5. Zaehle S, et al. (2010) Carbon and nitrogen cycle dynamics in the O-CN land surface model, II: The role of the nitrogen cycle in the historical terrestrial C balance. *Global Biogeochem Cycles* 24:1–14.
6. Krinner G, et al. (2005) Evaluation of ecosystem dynamics, plant geography and terrestrial carbon cycling in the LPJ dynamic global vegetation model. *Global Biogeochem Cycles* 19:1–33.
7. Cramer W, et al. (2001) Global response of terrestrial ecosystem structure and function to CO_2 and climate change: Results from six dynamic global vegetation models. *Glob Change Biol* 7:357–373.
8. Clark DB, et al. (2011) The Joint UK Land Environment Simulator (JULES), model description–Part 2: Carbon fluxes and vegetation dynamics. *Geosci Model Dev* 4:701–722.
9. Zeng N, Qian H, Roedenbeck C, Heimann M (2005) Impact of 1998–2002 midlatitude drought and warming on terrestrial ecosystem and the global carbon cycle. *Geophys Res Lett* 32:L22709.
10. New M, Hulme M, Jones P (1999) Representing twentieth-century space-time climate variability. Part I: Development of a 1961–90 mean monthly terrestrial climatology. *J Clim* 12:829–856.
11. New M, Hulme M, Jones P (2000) Representing twentieth-century space-time climate variability. Part II: Development of 1901–1996 monthly grids of terrestrial surface climate. *J Clim* 13:2217–2238.
12. New M, Lister D, Hulme M, Makin I (2002) A high-resolution data set of surface climate over global land areas. *Clim Res* 21:1–25.
13. Kalnay E, et al. (1996) The NCEP/NCAR 40-Year Reanalysis Project. *Bull Am Meteorol Soc* 77:437–471.
14. Le Quéré C, et al. (2014) Global carbon budget 2013. *Earth Syst. Sci. Data* 6:235–263.
15. MacFarling Meure C, et al. (2006) Law Dome CO_2, CH_4 and N_2O ice core records extended to 2000 years BP. *Geophys Res Lett* 33:L14810.
16. Keeling CD, et al. (2001) *Exchanges of Atmospheric CO_2 and $^{13}CO_2$ with the Terrestrial Biosphere and Oceans from 1978 to 2000. I. Global Aspects* (Scripps Inst Oceanogr, San Diego), SIO Ref Ser 01-06.
17. Gurney KR, et al. (2004) Transcom 3 Inversion Intercomparison: Control results for the estimation of seasonal carbon sources and sinks. *Global Biogeochem Cycles* 18:GB1010.
18. Stephens BB, et al. (2007) Weak northern and strong tropical land carbon uptake from vertical profiles of atmospheric CO_2. *Science* 316(5832):1732–1735.
19. Peylin P, et al. (2013) Global atmospheric carbon budget: Results from an ensemble of atmospheric CO_2 inversions. *Biogeosciences* 10:6699–6720.
20. Pan Y, et al. (2011) A large and persistent carbon sink in the world's forests. *Science* 333(6045):988–993.
21. Harris N, Brown S, Hagen S, Baccini A, Houghton R (2012) *Progress Toward a Consensus on Carbon Emissions from Tropical Deforestation: Policy Brief* (Meridian Inst, Washington, DC). Accessed March 1, 2014.
22. Tollefson J (2012) Scientists publish consensus statement on deforestation emissions. *Nat News Blog* Dec 4. Available at blogs.nature.com/news/2012/12/scientists-publish-consensus-statement-on-deforestation-emissions.html.
23. Baccini A, et al. (2012) Estimated carbon dioxide emissions from tropical deforestation improved by carbon- density maps. *Nat Clim Change* 2:182–185.

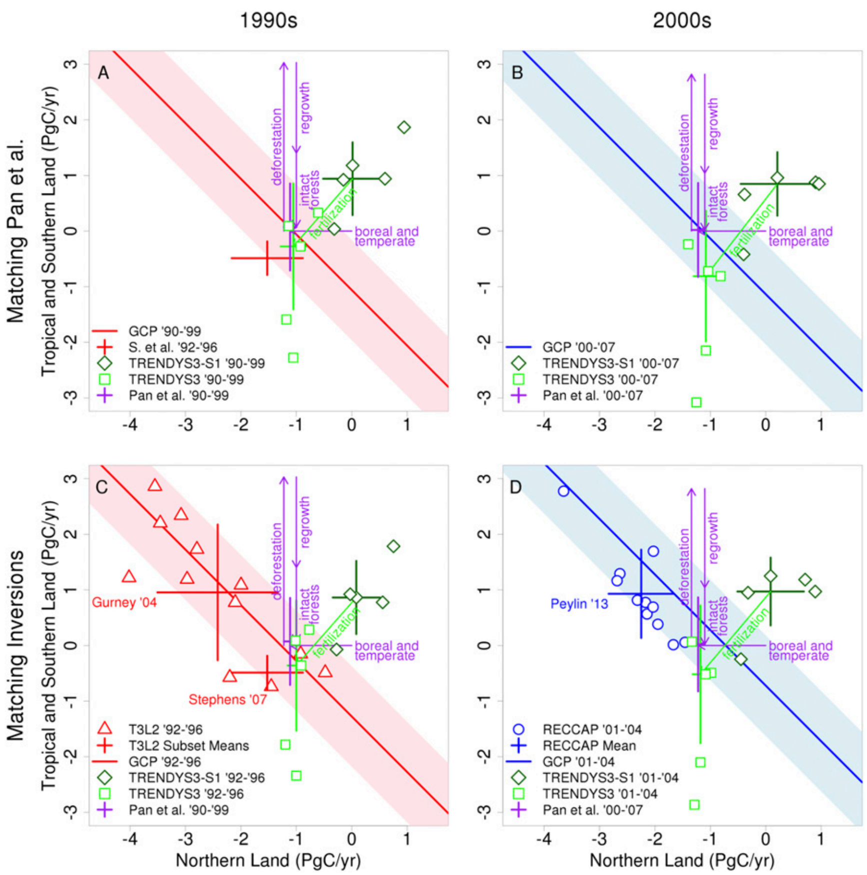

Fig. S1. Interdecadal variability: Results remain robust over four time periods. Flux estimates are made over varying time periods: T3L2 from 1992 to 1996, RECCAP from 2001 to 2004, TRENDY annually from 1901 to 2010, GCP annually from 1850 to 2012, and Pan et al. (20) decadally from 1990 to 2007. The 5-y and 4-y periods represented by T3L2 and RECCAP are likely to average over much interannual variability, but to address concerns about interannual variability, we have used the GCP budget and TRENDY output, which are available on an annual basis to examine comparisons on time periods matched to the shorter T3L2 or RECCAP periods and to the exact time periods captured by Pan et al. (20). These finer time periods support the conclusions from Fig. 3, that a significant CO_2 effect is needed to bring the TRENDY fluxes into agreement with the atmospheric inversion, global budget, and in situ inventory-based flux estimates, and that Pan et al. (20) generally lies outside the GCP constraint if uptake in intact forests is not included. The GCP results do not agree exactly with RECCAP or T3L2 on the fossil, ocean, and atmospheric accumulation values, leading to offsets between the inverse model and GCP results; (*A*) 1990–1999 for GCP, TRENDY, and Pan et al. (20), including Stephens et al. (18) (1992–1996); (*B*) 2000–2007 for all data sets; (*C*) 1992–1996, with Pan et al. (20) (1990–1999); and (*D*) 2001–2004 with Pan et al. (20) (2000–2007).

Table S1. The nine TRENDY (1) models, including five that reported S3 experiment results

Model	Spatial resolution, degrees lat x lon	S1 experiment global	S3 experiment northern extratropical land flux	S3 experiment tropical+southern land flux	S3 experiment tropical+southern land flux
CLM4CN	1.875 x 2.5	−1.41			
HYLAND	2.5 x 3.75	−3.25	−1.14	−2.63	−1.60
LPJ_GUESS	0.5 x 0.5	−2.56			
LPJwsl	0.5 x 0.5	−3.22	−0.70	−0.18	−0.19
OCN	2.5 x 3.75	−2.63	−0.98	−0.47	−0.54
ORCHIDEE	0.5 x 0.5	−4.63	−1.14	−1.84	−1.37
SDGVM	2.5 x 3.75	−2.18			
TRIFFID	2.5 x 3.75	−3.64			
VEGAS	2.5 x 2.5	−1.86	−1.26	−0.06	−0.04

Values include their spatial resolution, their 1990–2007 S1 Experiment (CO_2 only) fluxes, and their 1990–2007 northern extratropical and tropical+southern fluxes from the S3 Experiment (CO_2, climate, and land use). We also show the tropical contribution for reference. Region partitioning is according to the TransCom regions (see text). All flux units are petagrams carbon per year.

1. Piao S, et al. (2013) Evaluation of terrestrial carbon cycle models for their response to climate variability and to CO_2 trends. *Glob Change Biol* 19(7):2117–2132.

Table S2. The TransCom 3 Level 2 models and their 1992–1996 northern extratropical and tropical+southern land fluxes

Model	Northern extratropical land flux	Tropical+southern land flux	Tropical land flux
CSU	−3.55	2.86	3.30
GCTM	−2.00	1.09	2.75
UCB	−3.08	2.34	4.04
UCI	−1.45	−0.74	−0.08
JMA	−0.92	−0.15	−0.53
MATCH.CCM3	−2.10	0.77	2.31
MATCH.NCEP	−4.02	1.22	3.38
MATCH.MACCM	−2.97	1.19	2.48
NIES	−3.46	2.20	2.73
NIRE	−2.79	1.73	1.21
TM2	−0.48	−0.49	−0.96
TM3	−2.20	−0.57	0.99

Values are in petagrams carbon per year. We also show the tropical contribution for reference. Region partitioning is according to the TransCom regions (17).

Table S3. The RECCAP models and their 2001–2004 northern extratropical and tropical+southern land fluxes

Model	Northern extratropical land Flux	Tropical+southern land flux	Tropical land flux
LSCEa	−1.46	0.06	−0.19
MACC-II	−1.67	0.01	0.04
CCAM	−2.17	0.77	1.41
MATCH	−2.63	1.29	1.75
CT2011_oi	−2.14	0.57	0.25
CTE2013	−1.95	0.38	0.25
JENA (s96, v3.5)	−2.03	0.69	0.58
TrC	−2.68	1.17	1.67
RIGC (TDI-64)	−3.65	2.77	1.92
JMA	−2.31	0.81	0.13
NICAM	−2.03	1.69	2.88

Values are in petagrams carbon per year. We also show the tropical contribution for reference. Region partitioning is according to the TransCom regions (17).